JACS
JOURNAL OF THE AMERICAN CHEMICAL SOCIETY
Communication
pubs.acs.org/JACS

# Welding Molecular Crystals

Cyril R. R. Adolf, Sylvie Ferlay,* Nathalie Kyritsakas, and Mir Wais Hosseini*

Molecular Tectonics Laboratory, University of Strasbourg, UMR UdS-CNRS 7140, Institut Le Bel, 4 rue Blaise Pascal, 67000 Strasbourg, France

Supporting Information

**ABSTRACT:** Both for fundamental and applied sciences, the design of complex molecular systems in the crystalline phase with strict control of order and periodicity at both microscopic and macroscopic levels is of prime importance for development of new solid-state materials and devices. The design and fabrication of complex crystalline systems as networks of crystals displaying task-specific properties is a step toward smart materials. Here we report on isostructural and almost isometric molecular crystals of different colors, their use for fabrication of core−shell crystals, and their welding by 3D epitaxial growth into networks of crystals as single-crystalline entities. Welding of crystals by self-assembly processes into macroscopic networks of crystals is a powerful strategy for the design of hierarchically organized periodic complex architectures composed of different subdomains displaying targeted characteristics. Crystal welding may be regarded as a first step toward the design of new hierarchically organized complex crystalline systems.

The understanding and design of complex molecular systems in the crystalline phase with the control of the short- and long-range orders at the microscopic and macroscopic levels is important for both fundamental and applied sciences. Mastering molecular organization in the condensed phase is of prime importance for development of new solid-state materials and devices. Hierarchical interconnection of single crystals into supercrystals as "networks of crystals", for which specific subsections are interconnected with the continuation of the crystalline order, may be a powerful tool for generating hierarchically organized crystalline materials. Although welding of solid metallic materials is well-established, this process involving phase transition and occurring at high temperature and/or under pressure, leads to amorphous welded zones. Avoiding the loss of the ordered and periodic organization of matter within the welded zones requires the interconnection of crystals by crystalline phases. Welding individual crystals by self-assembly processes into macroscopic networks of crystals as single-crystalline entities is a powerful strategy for the design of hierarchically organized periodic complex architectures composed of different subdomains displaying specific characteristics. Crystal welding, an unexplored strategy, opens new directions in the design and fabrication of hierarchically organized complex matter. This approach, an example of crystal engineering,[1−3] may be regarded as a first step toward the design of new complex crystalline systems as networks of crystals displaying task-specific properties.

Here we report on the design of isostructural and almost isometric molecular crystals of different colors, their use for fabrication of core−shell crystals, and their welding into networks of crystals as crystalline entities by 3D epitaxial growth.

As stated by Dunitz, a molecular crystal may be seen as a periodic supramolecular entity[4] for which the components interact through reversible intermolecular interactions.[5] The molecular tectonics approach[6−8] is based on the design of tectons (construction units), their interaction through specific recognition events, and the repetition of the recognition processes under self-assembly conditions,[9] leading to molecular networks[10,11] displaying translational symmetry. For the molecular tectonics approach, all types of reversible intermolecular interactions ranging from weak van der Waals interactions to strong coordination bonds may be used to interconnect molecular tectons. Among many possible attractive interactions, rather weak but directional H bonding has been widely used for the design of molecular networks.[12] The strength of H-bonds may be further enhanced by adding an electrostatic charge−charge component (charge-assisted H bonding).[13,14] We have previously reported the design of H-bonded networks based on combinations of dicationic organic tectons of the cyclic bis-amidinium type as H-bond donors with anionic metal complexes as H-bond acceptor partners.[15] Taking advantage of the isostructural and almost isometric nature of a series of crystals, we have demonstrated the possibility of generating "crystals of crystals" or core−shell crystals by 3D epitaxial growth.[16−19] Few other examples of such hierarchical organization in the crystalline phase have been also reported.[20−22]

To generate isostructural and isometric crystals, we have combined the dicationic organic tecton $\mathbf{1}^{2+}$ with the anionic complex anion $[ML_2]^{4-}$ (M = Mn, Fe, Co, Ni, Cu, and Zn) as H-bond donor and acceptor, respectively (Figure 1). Tecton $\mathbf{1}^{2+}$, offering four acidic NH groups, behaving thus as a tetra H-bond donor, is based on two amidinium moieties interconnected by a phenyl spacer. The in situ formed metallatecton $[ML_2]^{4-}$, composed of a metal center in the oxidation state II complexed by two pyridinetricarboxylate ligands (L), should behave under the condition used as a tetra anionic H-bond acceptor partner. It is worth noting that the nature of the metal cation imposes the color of crystals. We have previously shown that combinations of the same organic tecton $\mathbf{1}^{2+}$ with dianionic

**Received:** October 16, 2015
**Published:** November 19, 2015




DOI: 10.1021/jacs.5b10586
J. Am. Chem. Soc. 2015, 137, 15390−15393

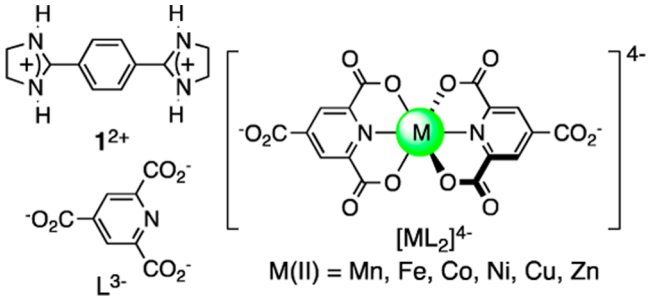


**Figure 1.** Tecton $\mathbf{1}^{2+}$, based on two cyclic amidinium moieties interconnected by a phenyl group as a tetra H-bond donor, trianionic pyridyl based ligand $L^{3-}$, and tetra anionic metallatectons $[M\text{-}L_2]^{4-}$ as a hexa H-bond acceptor. (b) Portion of the X-ray structure of $\mathbf{1}_2$-$ML_2$ crystals formed among tectons $\mathbf{1}^{2+}$, metallatectons $[ML_2]^{4-}$ (M = Mn, Fe, Co, Ni, Cu, and Zn), and water molecules. Except for the O atom of water molecules (colored green), H, C, N, O, and M atoms are colored in pink, gray, blue, red, and orange, respectively.

$[ML_2]^{2-}$ metallatectons leads to the formation of isostructural and almost isometric crystals. The latter feature was exploited for the generation of core−shell crystals.[19]

Combinations in solution of the dicationic tecton $\mathbf{1}^{2+}$ with anionic metallatecton $[ML_2]^{4-}$ (M = Mn, Fe, Co, Ni, Cu, and Zn) led to the formation of crystals displaying different colors (Figure 2).

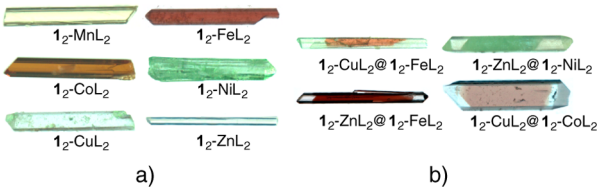


**Figure 2.** Photographs of (a) $\mathbf{1}_2$-$ML_2$ crystals obtained upon combining the dicationic tecton $\mathbf{1}^{2+}$ with anionic complexes $[ML_2]^{4-}$ (M = Mn, Fe, Co, Ni, Cu, and Zn) and (b) core−shell crystals $\mathbf{1}_2$-$M'L_2$@$\mathbf{1}_2$-$ML_2$ based on epitaxial growth of $\mathbf{1}_2$-$M'L_2$ crystals on $\mathbf{1}_2$-$ML_2$ seed crystals.

Structural investigations by X-ray diffraction on single crystals revealed that all combinations lead to isostructural and almost isometric nonporous $\mathbf{1}_2$-$ML_2$ single crystals (monoclinic system, $C2/c$ space group, $Z = 4$) with $a$, $b$, and $c$ cell dimensions in the 17.42−17.70, 20.04−21.15, and 13.70−13.84 Å ranges, respectively, with the $\beta$ value ranging from 101.7 to 102.7°. In all cases, crystals were composed of the tecton $\mathbf{1}^{2+}$ and the metallatecton $[ML_2]^{4-}$ (M = Mn, Fe, Co, Ni, Cu, and Zn), with a 2/1 tecton/metallatecton ratio for charge neutrality, and 10 water molecules. Positively and negatively charged components as well as water molecules are interconnected through H bonds and electrostatic interactions leading to a 3D cuboid-type architecture (Figure 3). For a detailed structural description, see the Supporting Information.

All six isomorphous crystalline materials obtained with different metal cations M (M = Mn, Fe, Co, Ni, Cu, and Zn) were also investigated by X-ray diffraction on microcrystalline powders. The observed diffraction patterns were compared to the simulated one. All crystalline materials display almost the same diffraction pattern indicating the presence of analogous single-phase crystalline powders. Good matches between the recorded and simulated patterns using single-crystal data were found for $\mathbf{1}_2$-$FeL_2$ (Figure 4). Discrepancies in intensity

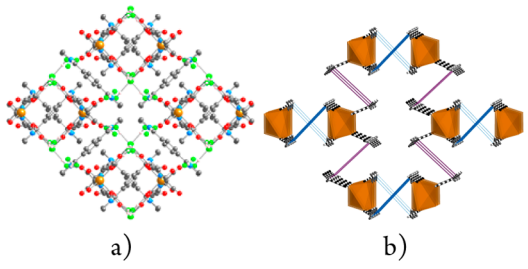


**Figure 3.** (left) Portion of the X-ray structure of $\mathbf{1}_2$-$ML_2$ crystals formed among tectons $\mathbf{1}^{2+}$, metallatectons $[ML_2]^{4-}$ (M = Mn, Fe, Co, Ni, Cu, and Zn), and water molecules. Except for the O atom of water molecules (colored green), H, C, N, O, and M atoms are colored in pink, gray, blue, red, and orange, respectively. (right) Corresponding schematized representation of the pseudocubic 3D H-bonded network. The dashed lines represent the hydrogen bonds, and the brown polyhedral are representing the $[M^{II}L_2]^{4-}$ metallatecton.

observed are due to preferential orientation of crystals within samples.

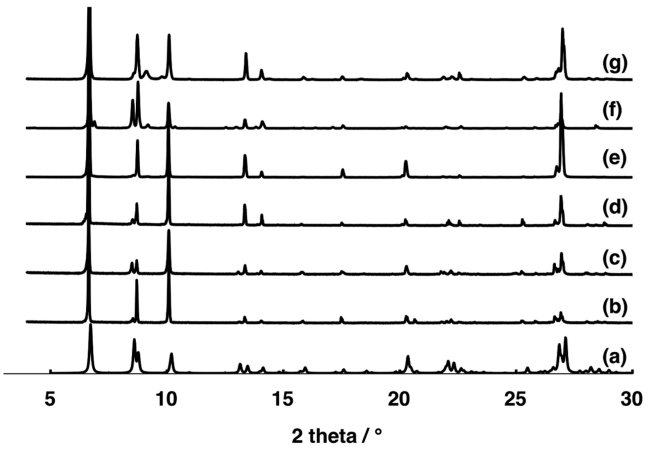


**Figure 4.** Comparison of PXRD patterns: (a) simulated for $\mathbf{1}_2$-$FeL_2$ and recorded for (b) $\mathbf{1}_2$-$FeL_2$, (c) $\mathbf{1}_2$-$MnL_2$, (d) $\mathbf{1}_2$-$CoL_2$, (e) $\mathbf{1}_2$-$NiL_2$, (f) $\mathbf{1}_2$-$CuL_2$, and (g) $\mathbf{1}$-$ZnL_2$. Discrepancies in intensity of peaks are due to preferential orientation of crystals within samples.

Crystal faces indexation revealed a preferential growth direction along the $z$ axis, in accordance with the rodlike shape of the obtained crystals (Figure 2).

As expected and stated above, the color of crystals (Figure 2a) depends on the nature of the metal cation M(II) composing the $[ML_2]^{4-}$ metallatecton (yellowish for Mn, orange for Fe, light-orange for Co, green for Ni, light-blue for Cu, and colorless for Zn). Taking advantage of the isostructural and almost isometric nature, robustness, and differences in color of $\mathbf{1}_2$-$ML_2$ crystals, the fabrication of $\mathbf{1}_2$-$M'L_2$@$\mathbf{1}_2$-$ML_2$ "crystals of crystals" or core−shell crystals was achieved by 3D epitaxial growth processes in solution (Figure 6a). A preformed $\mathbf{1}_2$-$ML_2$ seed crystal was immersed into a 9/1 $H_2O$/DMSO mixture containing the $\mathbf{1}$-2HCl, $L^{3-}$·3$Na^+$, and 0.5 equiv of $M'Cl_2$. (See the Supporting Information for details.) The growth process was monitored using a macroscope. The epitaxial growth leading to the core−shell crystals was completed within 6−8 h. It is worth noting that the rather flexible nature both in terms of distance and angle of H-bonding and electrostatic interactions allows for compensation for slight mismatches in unit cell parameters between the core



DOI: 10.1021/jacs.5b10586
J. Am. Chem. Soc. 2015, 137, 15390−15393

and shell crystals. The kinetics of growth is face-dependent and, as for the seed crystals, faster along the $z$ axis.

Four examples of core−shell crystals combining different M (Fe, Ni, and Co) and M′ (Cu and Zn) metal cations with the same organic tecton $\mathbf{1}^{2+}$ are given in Figure 2b. The hierarchically generated crystalline entities were investigated by X-ray diffraction methods, which revealed the continuity of the crystalline system through 3D epitaxial growth and the single-crystalline nature of core−shell materials.

Having established the possibility of generating core−shell crystals of the type $\mathbf{1}_2$-M′$L_2$@$\mathbf{1}_2$-M$L_2$, a further step of welding the crystals was explored. The welding process takes place in solution at room temperature and without any phase transition of the used components. Although many welding possibilities may be envisaged, here we shall focus on homo- and heterowelding as a proof of this unprecedented crystal welding concept.

Homowelding consists of cutting a crystal A into two parts. Both crystals were immobilized with a controlled distance between them and oriented along the fastest growth direction (along the $z$ axis, Figure 5b-i). The two separated entities were

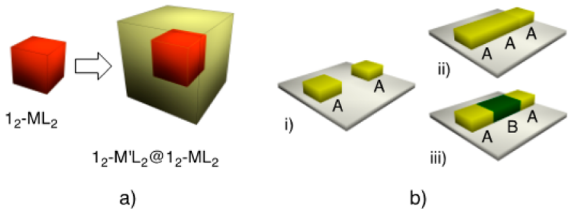


**Figure 5.** Schematic representation of (a) generation of a core−shell entity $\mathbf{1}_2$-M′$L_2$@$\mathbf{1}_2$-M$L_2$ resulting from 3D epitaxial growth of a crystalline $\mathbf{1}_2$-M′$L_2$ phase on a preformed $\mathbf{1}$-$_2$M$L_2$ crystal used as seed. (b) Welding of two crystals by a crystalline phase, leading to a single crystal composed of different crystalline zones. Homowelding of two crystals of A (i) by a crystalline phase A (ii), leading to a AAA welded crystal, and heterowelding of two crystals A (a) by a crystalline phase B (iii), leading to a ABA welded crystal.

immersed into a solution containing the same tecton $\mathbf{1}^{2+}$ and metallatecton $[ML_2]^{4-}$. The welding process results from epitaxial growth of a crystalline phase between the two identically oriented crystals. The welding procedure leads to a single crystal with the continuation of the crystalline system (Figure 5b-ii).

For heterowelding, the same procedure was applied. In this case, the two parts of crystal A were immersed into a solution containing the organic tecton $\mathbf{1}^{2+}$ and a different metallatecton $[M'L_2]^{4-}$. This procedure leads to a single crystal containing three different crystallographic domains (Figure 5b-iii).

Because preformed crystals were used as seed entities, an unsaturated welding solution was used to minimize nucleation and thus the growth of nonwelded single crystals. As stated above, the formation of rodlike crystals results from faster growth kinetics along the $z$ axis. This was used for the design of welding experiments. Rod-type preformed $\mathbf{1}_2$-M$L_2$ (M = Fe or Co) crystals were cut into two pieces (Figure 6a,d,g). In a Petri dish, both crystals were positioned with the same orientation along the $z$ axis with 45−255 $\mu$m distance between them (Figure 6b,e,h). At room temperature, they were covered with a drop of a 9/1 mixture of $H_2O$/DMSO containing the tecton $\mathbf{1}$-2HCl and ($L^{3-}$, $3Na^+$). The welding process was initiated upon addition of a drop of a 9/1 mixture of $H_2O$/DMSO containing 0.5 equiv of M′$Cl_2$ (M′ = Fe, Cu, or Ni) to the volume

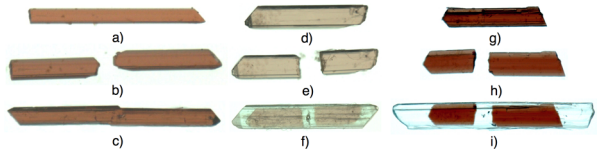


**Figure 6.** (a)Welding of $\mathbf{1}_2$-F$eL_2$ rodlike crystal, (b) its cutting leading to two crystals, and (c) their welding by $\mathbf{1}_2$-F$eL_2$ into a single crystal. (e) $\mathbf{1}_2$-F$eL_2$ rodlike crystal, (f) its cutting leading to two crystals, and (g) their welding by $\mathbf{1}_2$-Z$nL_2$ into a single crystal. (h) $\mathbf{1}_2$C$oL_2$ rodlike crystal, (i) its cutting leading to two crystals, and (j) their welding by $\mathbf{1}_2$-N$iL_2$ into a single crystal. All welded crystal were isolated and washed with distilled water.

containing the two crystals and the solution of $\mathbf{1}^{2+}$ and $L^{3-}$. The Petri dish was sealed, and the welding process monitored by a macroscope (Figure 6c,f,i). The speed of welding, as expected, was found to depend on the size of crystals and the distance between them. The welding was completed within 3 h in the case of homowelding (Figure 6c) of $\mathbf{1}_2$-F$eL_2$ crystals by $\mathbf{1}_2$-F$eL_2$ (distance between crystals of 45 $\mu$m), 8 h for heterowelding of $\mathbf{1}_2$-F$eL_2$ crystals by $\mathbf{1}_2$-Z$nL_2$ (Figure 6f, distance between crystals of 110 $\mu$m), and 48 h for heterowelding of $\mathbf{1}_2$-C$oL_2$ crystals by $\mathbf{1}_2$-N$iL_2$ (Figure 6i, distance between crystals of 255 $\mu$m). This corresponds to growth speed of ca. 15, 13, and 5 $\mu$m/h for (Fe−Fe−Fe), (Fe−Zn−Fe), and (Co−Ni−Co) cases, respectively. Depending on the size of crystals and the concentration of welding phases controlling the welding kinetics, the welded zone might contain some defects. For an example, see the recorded video for welding of $\mathbf{1}_2$-F$eL_2$ crystals by $\mathbf{1}_2$-Z$nL_2$ (Supporting Information).

All welded crystals reported were investigated by X-ray diffraction on single crystals. To structurally investigate the crystalline nature of the welded section, welded crystals were mounted on a goniometer, and the X-ray beam was alternatively focused on one of the two preformed crystal sections and on the welded zone. For each focusing procedure, frames were acquired and compared (Supporting Information). The unit cells parameters for both zones were determined and compared. In all three cases reported, they were found to be close to those determined for the pure phase.

It is worth mentioning that in nonconfined space 3D epitaxial growth takes place in all three directions of space. Thus, the welding process must also lead to core−shell type growth as discussed above. This was indeed observed because the welding process takes place only between two crystallographic faces arranged parallel to each other but also on the other faces of the oriented seed crystals (Figure 6).

It has been demonstrated that isostructural and almost isometric molecular crystals may be welded in solution by a 3D epitaxial growth process into a single-crystalline entity with the continuation of the crystalline order between the two welded crystals. The welding process may be of either homo (welding of two identical crystals by the same crystalline phase) or hetero (welding of two identical crystals by a different crystalline phase) nature. The formation of this type of entities validates the concept of welding molecular crystal by epitaxial growth leading to one single-crystal entity with different crystalline domains possessing each their own properties (color, magnetic, optical, porosity, etc.). The strategy presented here is a perfect example of crystal engineering.[1−3] It allows for mastering the organization of matter through hierarchical construction of macroscopic architectures and thus may be regarded as a first step toward the design of networks of crystals. This type of


DOI: 10.1021/jacs.5b10586
J. Am. Chem. Soc. 2015, 137, 15390−15393

hierarchical construction of periodic entities could open the way to the design of complex crystalline systems composed of different crystalline domains displaying task specific optical or magnetic properties. Further research along these lines are currently under investigation.

## ■ ASSOCIATED CONTENT

### Supporting Information

The Supporting Information is available free of charge on the ACS Publications website at DOI: 10.1021/jacs.5b10586.

Full experimental details (materials and techniques, synthesis, crystallization conditions, generation of crystals, experimental conditions for welding), crystallographic table for $1_2$-$ML_2$ crystals (M = Mn, Fe, Co, Ni, Cu, and Zn), description of crystal structures of $1_2$-$ML_2$, and characterization of welded crystals (frames and cell parameters). (PDF)

Video showing crystal growth. (AVI)

Crystallographic information files for $1_2$-$ML_2$ crystals (M = Mn, Fe, Co, Ni, Cu, and Zn). (ZIP)

## ■ AUTHOR INFORMATION


### Corresponding Authors

*ferlay@unistra.fr

*hosseini@unistra.fr


### Notes

The authors declare no competing financial interest.

## ■ ACKNOWLEDGMENTS

This work was supported in part by the University of Strasbourg, the CNRS, the International Center for Frontier Research in Chemistry (icFRC, Strasbourg), the Labex CSC (ANR-10-LABX- 0026 CSC) within the Investissement d'Avenir program ANR-10-IDEX-0002-02 and Institut Universitaire de France (IUF). We thank Professor J.-M. Lehn for financial support.

## ■ REFERENCES


(1) Schmidt, G. M. J. *Pure Appl. Chem.* **1971**, *27*, 647−678.

(2) Desiraju, G. D. *Crystal Engineering: The Design of Organic Solids*; Elsevier: New York, 1989.

(3) Desiraju, G. R. *Angew. Chem., Int. Ed. Engl.* **1995**, *34*, 2311−2327.

(4) Dunitz, J. D. *Pure Appl. Chem.* **1991**, *63*, 177−185.

(5) Lehn, J.-M. *Supramolecular Chemistry, Concepts and Perspectives*; VCH: Weinheim, Germany, 1995.

(6) Simard, M.; Su, D.; Wuest, J. D. *J. Am. Chem. Soc.* **1991**, *113*, 4696−4698.

(7) Mann, S. *Nature* **1993**, *365*, 499−505.

(8) Hosseini, M. W. *Acc. Chem. Res.* **2005**, *38*, 313−323.

(9) Whitesides, G. M.; Mathias, J. P.; Seto, T. *Science* **1991**, *254*, 1312−1319.

(10) Wells, A. F. *Three-Dimensional Nets and Polyhedra*; Wiley-Interscience: New York, 1997.

(11) Hosseini, M. W. *CrystEngComm* **2004**, *6*, 318−322.

(12) Etter, M. C. *Acc. Chem. Res.* **1990**, *23*, 120−126.

(13) Holman, K. T.; Pivovar, A. M.; Swift, J. A.; Ward, M. D. *Acc. Chem. Res.* **2001**, *34*, 107−118.

(14) Hosseini, M. W. *Coord. Chem. Rev.* **2003**, *240*, 157−166.

(15) Ferlay, S.; Hosseini, M. W. In *Functional Supramolecular Architectures for Organic Electronics and Nanotechnology*; Samori, P., Cacialli, F., Eds.; Wiley-VCH: Weinheim, Germany, 2001; Vol. *1*, pp 195−232.

(16) Ferlay, S.; Hosseini, M. W. *Chem. Commun.* **2004**, 788−789.

(17) Dechambenoit, P.; Ferlay, S.; Hosseini, M. W. *Cryst. Growth Des.* **2005**, *5*, 2310−2312.

(18) Dechambenoit, P.; Ferlay, S.; Kyritsakas, N.; Hosseini, M. W. *Chem. Commun.* **2009**, 1559−1561.

(19) Marinescu, G.; Ferlay, S.; Kyritsakas, N.; Hosseini, M. W. *Chem. Commun.* **2013**, *49*, 11209−11211.

(20) MacDonald, J. C.; Dorrestein, P. C.; Pilley, M. M.; Foote, M. M.; Lundburg, J. L.; Henning, R. W.; Schultz, A. J.; Manson, J. L. *J. Am. Chem. Soc.* **2000**, *122*, 11692−11702.

(21) Noveron, J. C.; Lah, M. S.; Del Sesto, R. E.; Arif, A. M.; Miller, J. S.; Stang, P. J. *J. Am. Chem. Soc.* **2002**, *124*, 6613−6625.

(22) Luo, T.-J. M.; MacDonald, J. C.; Palmore, G. T. R. *Chem. Mater.* **2004**, *16*, 4916−4927.




DOI: 10.1021/jacs.5b10586
*J. Am. Chem. Soc.* 2015, 137, 15390−15393